JYP

Molecular Docking and Prediction of Pharmacokinetic Properties of Dual Mechanism Drugs that Block MAO-B and Adenosine A_{2A} Receptors for the Treatment of Parkinson's Disease

Faizul Azam, Arwa M. Madi[1], Hamed I. Ali[2]

Department of Pharmaceutical Chemistry, NIMS Institute of Pharmacy, NIMS University, Jaipur, Rajasthan, India, [1]Department of Pharmaceutical Chemistry, Faculty of Pharmacy, Misurata University, Misurata, Libya, [2]Department of Pharmaceutical Chemistry, Helwan University, Ain Helwan, Cairo, Egypt

Address for correspondence: *Dr. Faizul Azam; E-mail: faizulazam@gmail.com*

ABSTRACT

Monoamine oxidase B (MAO-B) inhibitory potential of adenosine A_{2A} receptor ($AA_{2A}R$) antagonists has raised the possibility of designing dual-target–directed drugs that may provide enhanced symptomatic relief and that may also slow the progression of Parkinson's disease (PD) by protecting against further neurodegeneration. To explain the dual inhibition of MAO-B and $AA_{2A}R$ at the molecular level, molecular docking technique was employed. Lamarckian genetic algorithm methodology was used for flexible ligand docking studies. A good correlation (R^2 = 0.524 and 0.627 for MAO-B and $AA_{2A}R$, respectively) was established between docking predicted and experimental K_i values, which confirms that the molecular docking approach is reliable to study the mechanism of dual interaction of caffeinyl analogs with MAO-B and $AA_{2A}R$. Parameters for Lipinski's "Rule-of-Five" were also calculated to estimate the pharmacokinetic properties of dual-target–directed drugs where both MAO-B inhibition and $AA_{2A}R$ antagonism exhibited a positive correlation with calculated Log*P* having a correlation coefficient R^2 of 0.535 and 0.607, respectively. These results provide some beneficial clues in structural modification for designing new inhibitors as dual-target–directed drugs with desired pharmacokinetic properties for the treatment of PD.

Key words: Adenosine A_{2A} antagonist, docking, dual-target–directed drugs, monoamine oxidase B

INTRODUCTION

Parkinson's disease (PD) is primarily a disorder of the nigrostriatal dopaminergic pathway that results in the cardinal motor symptoms of bradykinesia, tremor, and rigidity.[1] Nondopaminergic treatments are increasingly being recognized as part of the therapeutic armamentarium for PD,[2-7] because long-term treatment with dopamine replacement strategies is associated with drug-related complications, such as a loss of drug efficacy, the onset of dyskinesias, and the occurrence of psychosis and depression.[8] Therefore, development of suitable approach to the treatment of this devastating neurodegenerative disorder remains an indispensable component of research in medicinal chemistry. Nowadays, an emerging paradigm that proposes the targeting

Access this article online	
Quick Response Code:	Website: www.jyoungpharm.in
	DOI: 10.4103/0975-1483.100027

of multiple components of pathobiology through a single drug molecule is gaining increasing acceptance. Although the single-target or "silver bullet" approach currently remains the major drug discovery strategy in large pharmaceutical companies, there is increasing recognition of the limitations of such an approach for complex diseases.

Monoamine oxidase B (MAO-B) is an outer membrane–bound mitochondrial flavoenzyme that functions in the oxidative deamination of dopamine in the striatum.[9] Inhibition of MAO-B in the brain may slow the depletion of dopamine stores and elevate the levels of endogenous dopamine, and dopamine produced from exogenously administered levodopa.[10,11] Furthermore, inhibitors of the MAO-B may also exert a neuroprotective effect by decreasing the production of potentially hazardous byproducts of dopamine metabolism in the brain.[12] Adenosine A_{2A} receptor ($AA_{2A}R$) antagonists are another class of promising anti-Parkinsonian agents and a leading candidate class for the nondopaminergic treatment of symptomatic PD.[6] $AA_{2A}R$ antagonists may also possess neuroprotective properties and may prevent the development of dyskinesia that is usually associated with levodopa treatment.[13,14] Interestingly, it has been observed that $AA_{2A}R$ antagonists also inhibit MAO-B; therefore, they can be exploited in designing dual-target–directed drugs aimed at providing enhanced symptomatic relief in addition to slowing the progression of PD by protecting against further neurodegeneration.[15] In this regard, C8-substituted caffeinyl derivatives are becoming popular as dual-target–directed drugs that block MAO-B and $AA_{2A}R$ for the treatment of PD.

Significant progress has been made in computer-aided drug design by pharmaceutical companies at different stages of drug discovery, such as identifying new hits, enhancing molecule binding affinity in hit-to-lead, and lead optimization.[16] Moreover, *in silico* approaches are routinely used in modern drug design to help understand drug–receptor interactions. It has been shown in the literature that computational techniques can strongly support and help the design of novel, more potent inhibitors by revealing the mechanism of drug–receptor interactions.[17] However, so far, there has been no report concerning the application of molecular docking methodology for understanding the binding of dual-target–directed drugs that block MAO-B and $AA_{2A}R$. To gain an insight into the structural requirements for the dual inhibition, we have used molecular docking studies to understand the mode of binding of C8-substituted caffeinyl analogs to MAO-B and $AA_{2A}R$. In addition, we have also employed computational method for the determination of physicochemical parameters that are responsible for governing the pharmacokinetic properties of drug molecules. For the present study, $AA_{2A}R$ antagonists with MAO-B inhibitory properties were taken from the literature[15,18-24] and subjected to *in silico* studies. The results obtained from this study would be useful in both understanding the inhibitory mode of these derivatives as well as in rapidly and accurately predicting the activities of newly designed inhibitors. Some beneficial clues can also be inferred from these results that will be fruitful in designing novel inhibitors as dual-target–directed drugs with desired pharmacokinetic properties in the area of PD therapeutics.

MATERIALS AND METHODS

For the present study, crystal structures of human MAO-B (PDB code: 2V5Z)[25] and human $AA_{2A}R$ (PDB code: 3EML)[26] were downloaded from the protein databank (www.rcsb.org/pdb). A set of 18 inhibitors [Table 1] that inhibit MAO-B and antagonize $AA_{2A}R$ were taken from the literature[15,18-24] and docked onto the active site of MAO-B and $AA_{2A}R$ using AutoDock 4.2 (Release 4.2.2.1) program.

Molecular docking studies

For docking experiments with AutoDock 4.2, ligand molecules were drawn in ChemBioDraw Ultra 12.0 and converted to their 3-dimensional structures in ChemBio3D Ultra 12.0, energy minimized by PM3 method using MOPAC Ultra 2009 program.[27] The prepared ligands were used as input files for AutoDock 4.2 in the next step. Lamarckian genetic algorithm method was employed for docking simulations.[28] The standard docking procedure was used for a rigid protein and a flexible ligand whose torsion angles were identified (for 10 independent runs per ligand). A grid of 60, 60, and 60 points in x, y, and z directions was built with a grid spacing of 0.375 Å and a distance-dependent function of the dielectric constant were used for the calculation of the energetic map. The default settings were used for all other parameters. At the end of docking, the best poses were analyzed for hydrogen bonding/π–π interactions and root mean square deviation (RMSD) calculations using Discovery Studio Visualizer 2.5 program. From the estimated free energy of ligand binding ($\Delta G_{binding}$, kcal/mol), the inhibition constant (K_i) for each ligand was calculated [Tables 2 and 3].

Calculation of physicochemical parameters

Absorption (%ABS) was calculated by: %ABS = 109 – [0.345 × topological polar surface area (TPSA)] according

to the method of Zhao *et al*.[29] TPSA,[30] miLog*P*, number of rotatable bonds, and violations of Lipinski's "Rule-of-Five"[31] were calculated using Molinspiration online property calculation toolkit.[32]

RESULTS AND DISCUSSION

Molecular docking

Validation of the accuracy and performance of AutoDock 4.2

To validate the accuracy of AutoDock 4.2 as an appropriate docking tool for the present purpose, the co-crystallized ligands (Safinamide and ZM241385 for 2V5Z.pdb and 3EML.pdb, respectively) were docked within the inhibitor-binding cavity (IBC) of human MAO-B and human $AA_{2A}R$, and the docked position was compared with the crystal structure position by calculating RMSD values (1.27 and 0.88 Å, respectively). As a general rule, if the best-docked conformation of a ligand resembles the bound native ligand in the experimental crystal structure, the used scoring function is said to be successful. According to the method of validation cited in the literature,[33] the successful scoring function is the one in which the RMSD of the best docked conformation is ≤2.0 Å from the experimental one. In this study, RMSD values of both MAO-B and $AA_{2A}R$ were within 2.0 Å [Figure 1], indicating our docking methods are valid for the given structures and AutoDock 4.2, therefore deemed reliable for docking dual-target–directed drugs into the IBC of MAO-B and $AA_{2A}R$.

Docking of the caffeinyl analogs into $AA_{2A}R$

The co-crystallized $AA_{2A}R$ antagonist, ZM241385, is outlined by Leu-85, Phe-168, Glu-169, Met-177, Trp-246, Leu-249, His-250, Asn-253, His-264, Leu-267, and Met-270 residues, which constitute the active binding site.[26] The poor affinity of caffeine (compound 1) toward $AA_{2A}R$ in experimental studies can be clearly explained on the basis of our docking results as shown in Figure 2, where none of the residues of binding site was found to interact with caffeine neither in terms of hydrophobic nor hydrophilic interactions. However, in close proximity of the binding cavity, it interacted with His-278 by forming a hydrogen bond. It was interesting to note that the xanthine nucleus orients inside the binding cavity and interacts by both

Table 1: The structures, *Ki* and p*Ki* values for MAO-B inhibition and $AA_{2A}R$ antagonism by 8-substituted caffeinyl analogs

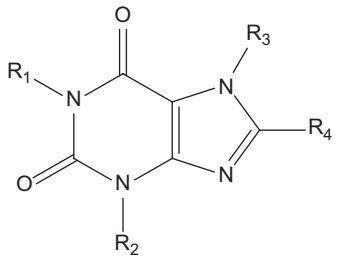

Compounds	R_1	R_2	R_3	R_4	MAO-B		$AA_{2A}R$	
					K_i	pK_i	K_i[3]	pK_i
1	Me	Me	Me	H	3.6 [1,a]	2.44	22000[b]	4.66
2	Me	Me	Me	3-Chlorostyryl	0.235 [2,c]	6.63	54[d]	7.28
3	Et	Et	Me	3,4-Dimethoxystyryl	17 [2,c]	4.77	4.46[e]	8.35
4	Et	Et	H	3,4-Dimethoxystyryl	63 [2,c]	4.20	23[f]	7.64
5	Me	Me	H	3,4-Dimethoxystyryl	6 [2,c]	5.22	1100[d]	5.96
6	Me	Me	Me	3,4-Dimethoxystyryl	2.7 [2,c]	5.57	197[d]	6.71
7	Me	Me	H	3-Nitrostyryl	9 [2,c]	5.05	438[d]	6.36
8	Me	Me	Me	Styryl	3 [2,c]	5.52	94[d]	7.03
9	Me	Me	H	Styryl	31 [2,c]	4.51	291[d]	6.54
10	Me	Me	H	3-Fluorostyryl	1.9 [2,c]	5.72	516[d]	6.29
11	Me	Me	Me	3-Nitrostyryl	0.16 [2,c]	6.80	195[d]	6.71
12	Me	Me	Me	3-Fluorostyryl	0.4 [2,c]	6.40	83[d]	7.08
13	Et	Et	Me	3,4-Methylenedioxystyryl	8 [2,c]	5.10	6.1[f]	8.21
14	Me	Me	Me	4-phenylbutadien-1-yl	148.6 [3,g]	6.83	153[h]	6.82
15	Me	Me	Me	4-(3-chlorophenyl)butadien-1-yl	42.1 [3,g]	7.38	104[h]	6.98
16	Me	Me	Me	4-(3-bromophenyl)butadien-1-yl	17.2 [3,g]	7.76	59.1[h]	7.23
17	Me	Me	Me	4-(3-fluorophenyl)butadien-1-yl	46.4 [3,g]	7.33	114[h]	6.94
18	Me	Me	Et	4-phenylbutadien-1-yl	1712 [3,g]	5.77	13.5[h]	7.87

MAO-B, monoamine oxidase B; $AA_{2A}R$, adenosine A_{2A} receptor; K_i, experimentally determined inhibition constant; pK_i, negative logarithm of K_i. [1] Value given in mM. [2] Values given in µM. [3] Values given in nM. [a, b, c, d, e, f, g, h]Experimental K_i taken from Refs. 15 and 18–24 respectively.

hydrophobic as well as hydrophilic interactions when C-8 position is substituted with (*E*)-styryl and 4-phenylbutadien-1-yl groups making these compounds fairly potent [Figure 3].

The bicyclic triazolotriazine core of ZM241385 is anchored by an aromatic stacking interaction with Phe-168,[34] an aliphatic hydrophobic interaction with Ile-274[13,35] and a hydrogen bonding interaction with Asn-253.[36,37] Likewise, the bicyclic xanthine ring was found to interact with aromatic ring of Phe-168 by π–π stacking interaction while Asn-253 contributed in hydrophilic interaction by forming a hydrogen bond. A report by Moro *et al*. has also proposed that the bicyclic ring of ZM241385 is anchored by hydrophobic interactions of Leu-249.[38] Adjacent to Phe-168, a polar residue Glu-169 shares a hydrogen bond with the oxygen atom of 3,4-methylenedioxy group. Similar kind of interaction is also known between exocyclic amino group (N15 atom) linked to the bicyclic core of ZM241385.[34,39]

Docking of the caffeinyl analogs into MAO-B

The docked compounds 1–18 oriented into the IBC of MAO-B and $AA_{2A}R$ in a similar way as their native ligands safinamide and ZM241385 interact with MAO-B[25] and $AA_{2A}R$,[26] respectively, exhibiting a reasonable RMSD values in the range of 0.37–6.17 Å. The reported and estimated inhibition constant (K_i) was converted to their respective pK_i (–log K_i) and plotted as shown in Figure 4. A positive correlation was noted between docking predicted and experimentally reported pK_i with a correlation

Table 2: Results obtained after docking of 8-substituted caffeinyl analogs with human MAO-B

Compounds	ΔG_b[a]	K_i[b]	pK_i[c]	RMSD[d] (Å)	π-interactions		H-bond interactions		
					Amino acids	Distance (Å)	Compound	Amino acids	Distance (Å)
1	−6.26	25.90[1]	4.59	4.38	Tyr-398	3.97	O	Tyr-188	2.74
							O	Tyr-435	3.09
2	−8.78	367.61[2]	6.44	2.89	Tyr-398	3.99	O	Tyr-188	2.82
					Tyr-398	4.45	O	Tyr-435	2.93
3	−7.85	1.77[1]	5.75	1.13	—[e]	—	O	Gln-206	2.75
							O	Tyr-326	3.19
4	−8.14	1.08[1]	5.97	1.70	—[e]	—	O	Gln-206	3.13
							O	Tyr-326	2.53
5	−8.99	256.59[2]	6.59	1.39	—[e]	—	O	Gln-206	2.91
							O	Tyr-326	2.86
6	−8.44	646.65[2]	6.19	4.72	—[e]	—	O	Cys-172	3.10
							O_4	Thr-201	2.89
							O_3	Thr-201	2.41
							O_2	Gln-206	3.19
7	−5.72	64.37[1]	4.19	2.24	—[e]	—	O_2	Phe-168	2.71
							O_3	Tyr-398	2.79
							O_4	Tyr-398	2.35
8	−7.87	1.71[1]	5.77	4.16	—[e]	—	O	Cys-172	3.18
9	−7.92	1.56[1]	5.81	4.23	—[e]	—	N	Ile-199	2.86
							O	Gln-206	2.22
10	−7.87	1.71[1]	5.77	4.32	Pro-102	5.95	O	Cys-172	3.21
							O	Gln-206	2.50
							O	Tyr-326	3.09
							N	Ile-199	2.86
11	−7.81	1.89[1]	5.72	1.47	Tyr-398	5.40	O_4	Tyr-326	2.69
12	−7.77	2.02[1]	5.69	4.28	—[e]	—	O_2	Cys-172	3.19
							F	Thr-201	2.84
13	−7.71	2.25[1]	5.66	1.06	—[e]	—	N_2	Cys-172	3.21
							O_2	Gln-206	2.79
							O_2	Tyr-326	3.04
14	−9.76	70.69[2]	7.15	1.85	—[e]	—	O	Cys-172	3.12
15	−11.45	4.04[2]	8.39	0.37	Tyr-398	4.31	O_2	Tyr-188	2.80
					Tyr-398	5.64			
16	−11.96	1.71[2]	8.77	0.52	Tyr-398	4.21	O_{14}	Tyr-188	2.76
					Tyr-398	5.49			
17	−9.85	59.94[2]	7.22	2.25	Tyr-398	4.60	O_2	Tyr-188	3.06
					Tyr-398	3.95	O	Tyr-435	2.83
18	−10.31	27.66[2]	7.56	1.61	—[e]	—	O	Cys-172	3.00
Safinamide	−9.81	64.08[2]	7.19	1.27	—[e]	—	N_{21}	Gly-434	3.14
							O_{20}	Tyr-188	1.97

[a]Binding free energy (kcal/mol). [b]Docking predicted inhibition constant. [c]Negative logarithm of docking predicted inhibition constant. [d]Root mean square deviation. [e]No π-interactions. [1]Values given in μM [2]Values given in nM

coefficient R^2 of 0.524 and 0.627 for MAO-B and $AA_{2A}R$, respectively.

The caffeinyl derivatives docked into the IBC of human MAO-B was outlined by residues, such as Pro-102, Leu- 171, Cys-172, Ile-198, Ile-199, Gln-206, Ile-316, Tyr- 326, Phe-343, Tyr-398, Tyr-435, and the isoalloxazine ring of FAD.[40] The major part of the IBC is hydrophobic, which allows for the tight binding of nonpolar substrates and inhibitors.[41] This is the reason why the calculated Log*P* presented in Table 4 bears a positive correlation with the MAO-B inhibitory activity exhibiting a correlation coefficient R^2 of 0.535 [Figure 4]. However, the only hydrophilic portion is near the flavin and is required for recognition and directionality of the substrate amine functionality.[41] This hydrophilic region is located between Tyr-398 and Tyr-435, which, together with the flavin, form an aromatic cage for amine recognition.[42,43] Moreover, Gln-206 interacts by forming a hydrogen bond with the native co-crystallized ligand, safinamide. In a similar way, Gln-206 serves as hydrogen bond acceptor for most of the docked compounds [Figure 5].

In addition to contributing for hydrophobicity in the IBC, Phe-168, Cys-172, Ile-199, Thr-201, and Tyr-326 were also appeared to participate in hydrogen bond formation. Interestingly, (E)-8-(3-chlorostyryl) caffeine (CSC, compound 2) and compounds containing 4-phenylbutadien-1-yl groups at C-8 position of the caffeinyl moiety were observed to share a hydrogen bond with Tyr-188, a residue located at the distant site in the IBC.

Table 3: Results obtained after docking of 8-substituted caffeinyl analogs with human $AA_{2A}R$

Compounds	ΔG_b[a]	K_i[b]	pK_i[c]	RMSD[d] (Å)	π-Interactions		H-bond interactions		
					Amino acids	Distance (Å)	Compound	Amino acids	Distance (Å)
1	−5.06	196.90[2]	3.71	6.13	—[e]	—	O_2	His-278	2.00
2	−7.96	1.45[2]	5.84	4.31	Phe-168	4.86	O	Asn-253	2.02
					Phe-168	4.16			
3	−8.15	1. 06[1]	5.98	1. 32	Phe-168	3.59	O_4	Glu-169	2.2
					Phe-168	4.04	O_2	Asn-253	2.23
4	−8.41	683.20[3]	6.17	2.74	—[e]	—	O_3	Phe-168	2.43
							O_4	Glu-169	1.83
							O_2	His-278	2.29
5	−7.98	1.42[2]	5.85	3.87	Phe-168	3.75	O_3	Asn-253	1.78
							O_2	His-278	2.10
6	−7.91	1.58[2]	5.80	1.01	Phe-168	3.59	O	Glu-169	1.97
					Phe-168	3.98		Asn-253	2.07
7	−7.11	6.18[2]	5.21	4.40	—[e]	—	O_3	Val-84	1.82
8	−7.52	3.08[2]	5.51	4.24	Phe-168	4.83	O	Asn-253	1.99
					Phe-168	4.06			
9	−7.33	4.26[2]	5.37	4.70	Phe-168	4.34	O_2	Asn-253	2.04
					Phe-168	3.62			
10	−7.20	5.30[2]	5.28	4.70	Phe-168	4.34	O_2	Asn-253	2.04
					Phe-168	3.62			
11	−8.29	835.19[3]	6.08	4.54	—[e]	—	O_2	Phe-168	1.90
							O_3	His-278	1.97
12	−7.47	3.36[2]	5.47	4.24	Phe-168	4.82	O_2	Asn-253	1.96
					Phe-168	4.07	F	His-278	50
13	−8.32	797.11[3]	6.10	0.99	Phe-168	4.08	O_4	Glu-169	2.11
					Phe-168	3.66	O	Asn-253	2.01
14	−8.20	972.46[3]	6.01	2.58	Phe-168	4.02	O_2	Asn-253	1.90
					Phe-168	3.88			
15	−7.78	1.98[2]	5.70	2.95	—[e]	—	—	—	—
16	−8.44	645.77[3]	6.19	3.10	—[e]	—	O_{13}	His-278	2.02
17	−8.09	1.18[2]	5.93	4.70	Phe-168	4.48	O	Asn-253	2.17
					Phe-168	5.15			
18	−8.40	697.38[3]	6.16	2.72	Phe-168	3.99	O_2	Asn-253	1.91
					Phe-168	3.87			
ZM241385	−8.21	964.13[3]	6.02	0.88	Phe-168	3.93	H_1	Ile-66	2.42
					Phe-168	4.03	H_3	Asn-253	2.34
							H_4	Glu-169	1.88
							H_5	Asn-253	1.69
							O_{25}	Asn-253	2.07

[a]Binding free energy (kcal/mol). [b]Docking predicted inhibition constant. [c]Negative logarithm of docking predicted inhibition constant. [d]Root mean square deviation.
[e]No π-interactions. [1]Values given in mM. [2]Values given in μM. [3]Values given in nM.

Likewise, 4-phenylbutadien-1-yl derivatives also interact with Tyr-435, a residue found in the hydrophilic region of the IBC [Table 2].

Caffeine, being a polar compound, is not able to accommodate well in the IBC and is a weak MAO-B inhibitor. However, substitution of the (*E*)-styryl and 4-phenylbutadien-1- yl groups at C-8 markedly decreases the polarity of the molecule as reflected by the high calculated Log*P* of these compounds [Table 4] appears to be beneficial for the MAO-B inhibitory activity. On the other hand, it is known that the active site of the MAO-B consists of an entrance connected to the substrate cavity where Ile-199 acts as a "gate" between the two cavities. When relatively large inhibitors, such as the reversible inhibitor 1,4-diphenyl-2-butene is bound, the side chain is rotated to a conformation such that the two cavities are no longer separated and are now fused forming a single cavity and such compounds demonstrate greater binding affinity.[41] Our docking results reflect that (*E*)-styryl and 4-phenylbutadien-1-yl groups at C-8 position of the

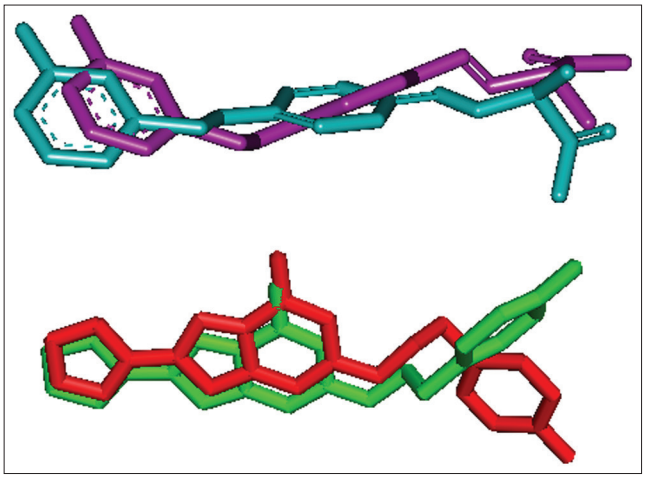

Figure 1: The validation of accuracy and performance of AutoDock 4.2. The docked safinamide (purple) and native safinamide (cyan) demonstrated a root mean square deviation of 1.27 Å, whereas the docked ZM241385 (red) and native ZM241385 (green) exhibited a root mean square deviation of 0.88 Å

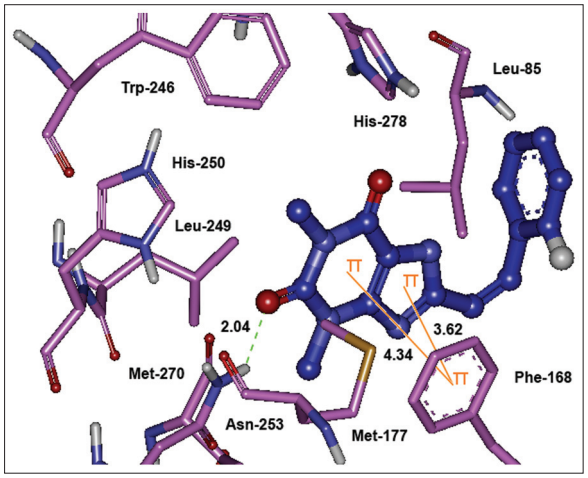

Figure 3: The lowest energy configuration of docking result of caffeinyl analog (Compound 10) with binding pocket of human $AA_{2A}R$. The residues of binding pocket are shown as stick in pink color while compound 10 is presented as ball and stick style in blue color. Dashed lines in green indicate H-bonds while π–π stacking interaction are shown as orange lines. Sulfur is presented in dark yellow and oxygens in red

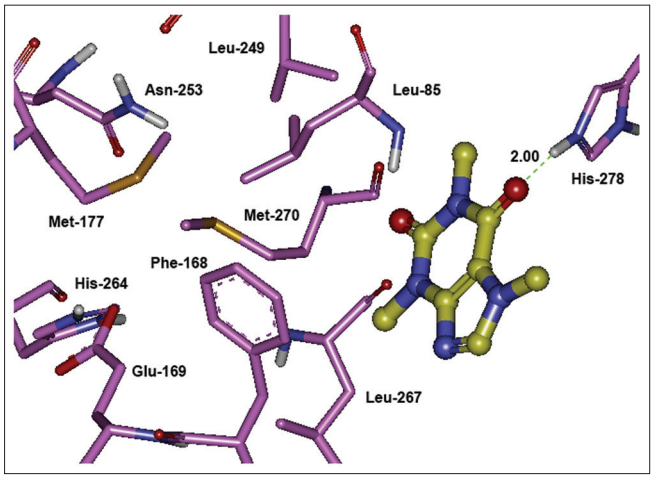

Figure 2: The lowest energy configuration of docking result of caffeine with binding pocket of human $AA_{2A}R$. The residues of binding pocket are shown as stick in pink color, and caffeine is presented as ball and stick style in yellow color. Dashed lines in green indicate H-bonds. Nitrogens are in blue and oxygens are in red

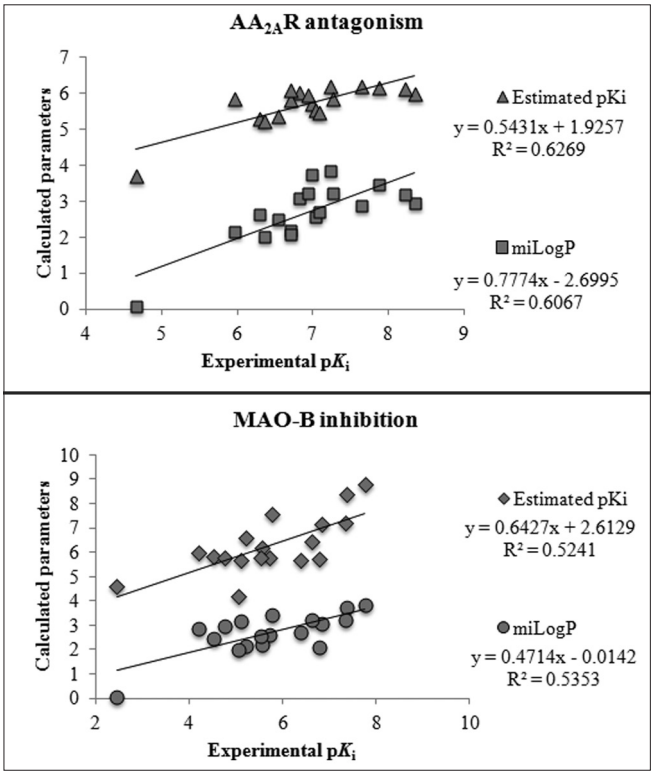

Figure 4: Experimental pK_i is plotted against docking estimated pK_i, and miLog*P*

caffeinyl moiety use both cavities as potential binding targets making them potent MAO-B inhibitors. Similarly, without the side chain at C-8, caffeine occupies only hydrophilic region leaving the hydrophobic region unoccupied and hence exhibits less binding affinity [Figure 6]. Based on these results, an overview of the structural requirements for antagonizing $AA_{2A}R$ and inhibiting MAO-B is presented in Figure 7.

Physicochemical parameters

Among xanthine-based $AA_{2A}R$ antagonists, poor water solubility is a considerable problem.[6] Lipinski's parameters[31] were calculated by using Molinspiration online property calculation toolkit[32] to estimate the pharmacokinetic properties of caffeinyl derivatives (1–18) and presented in Table 4. Topological polar surface area (TPSA), that is, surface belonging to polar atoms, is a descriptor that was shown to correlate well with passive molecular transport through membranes and, therefore, allows prediction of transport properties of drugs in the intestines and blood–brain barrier crossing.[30] TPSA was used to calculate the percentage of absorption (%ABS) according to the equation: %ABS = 109 − 0.345 × TPSA, as reported by Zhao *et al*.[29] Furthermore, according to Veber *et al*., good bioavailability is more likely for compounds with ≤10 rotatable bonds and TPSA of ≤140 Å^2.[44] As the number of rotatable bonds increases, the molecule becomes more flexible and more adaptable for efficient interaction with a particular binding pocket. In the present study, compounds 1–18 exhibited % ABS ranging from 68% to 87%, which is an indication of good bioavailability by oral route. Moreover, nonviolations of Lipinski's "Rule-of-Five" and

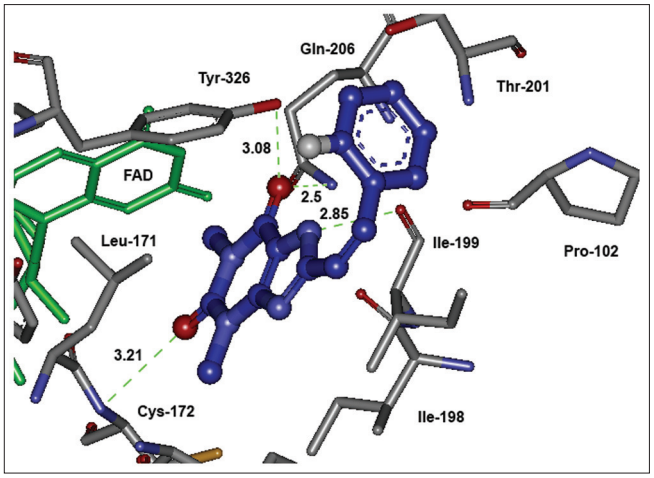

Figure 5: The lowest energy configuration of docking result of caffeinyl analog (Compound 10) with binding pocket of human MAO-B. The amino acids (gray) and FAD (green) are shown as stick while compound 10 is presented as ball and stick style in blue color. Dashed lines in green indicate H-bonds. Sulfur is presented in dark yellow and oxygens in red

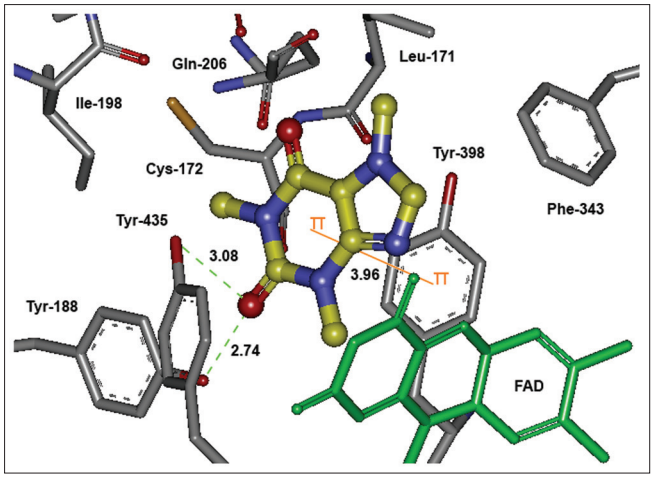

Figure 6: The lowest energy configuration of docking result of caffeine with binding pocket of human MAO-B. The amino acids (gray) and FAD (green) are shown as stick while caffeine is presented as ball and stick style in yellow color. Dashed lines in green indicate H-bonds while π–π stacking interaction is shown as orange line. Nitrogens are in blue and oxygens in red

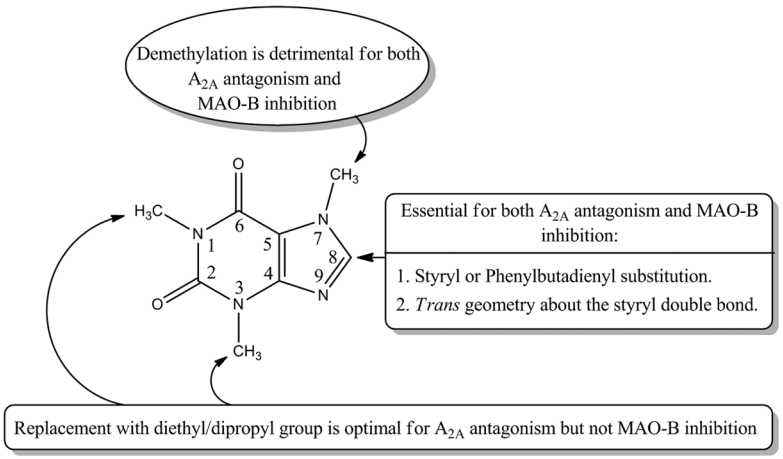

Figure 7: An overview of the structural requirements for antagonizing $AA_{2A}R$ and inhibiting MAO-B

Table 4: Physicochemical parameters for good oral bioavailability of caffeinyl analogs

Compounds	%ABS[a]	TPSA (Å^2)[b]	MW[c]	miLog*P*[d]	HBD[e]	HBA[f]	n-ROTB[g]	Lipinski's violation
Rule	—	—	<500	≤5	<5	<10	≤10	≤1
1	87.67	61.84	194.19	0.06	0	6	0	0
2	87.67	61.84	330.78	3.2	0	6	2	0
3	81.3	80.30	384.44	2.95	0	8	6	0
4	77.55	91.16	370.41	2.88	1	8	6	0
5	77.55	91.16	342.36	2.13	1	8	4	0
6	81.3	80.30	356.38	2.19	0	8	4	0
7	68.11	118.52	341.33	2.01	1	9	3	0
8	87.67	61.84	296.33	2.55	0	6	2	0
9	83.92	72.69	282.31	2.48	1	6	2	0
10	83.92	72.69	300.29	2.62	1	6	2	0
11	71.86	107.66	355.35	2.08	0	9	3	0
12	87.67	61.84	314.32	2.69	0	6	2	0
13	81.3	80.30	368.39	3.19	0	8	4	0
14	87.67	61.84	322.37	3.07	0	6	3	0
15	87.67	61.84	356.81	3.72	0	6	3	0
16	87.67	61.84	401.26	3.85	0	6	3	0
17	87.67	61.84	340.36	3.21	0	6	3	0
18	87.67	61.84	336.39	3.44	0	6	4	0

[a]Percentage of absorption. [b]Topological polar surface area. [c]Molecular weight. [d]Logarithm of compound partition coefficient between *n*-octanol and water. [e]Number of hydrogen bond donors. [f] Number of hydrogen bond acceptors. [g]Number of rotatable bonds.

Veber's "criteria for good bioavailability" also confirm the suitability of these compounds to be used as a template for the design of dual-target–directed drugs.

CONCLUSION

In conclusion, these computational studies not only shed a light on understanding the dual mechanism of MAO-B inhibition as well as $AA_{2A}R$ antagonism, but also provide precious insight for the rational improvements of specificity and inhibitory potency of C-8 substituted caffeinyl analogs to be explored as novel anti-Parkinsonian drug candidates.

REFERENCES

1. Abou-Sleiman PM, Muqit MM, Wood NW. Expanding insights of mitochondrial dysfunction in Parkinson's disease. Nat Rev Neurosci 2006;7:207-19.
2. Azam F. Synthesis of some urea and thiourea derivatives of naphtha[1,2-*d*] thiazol-2-amine as anti- Parkinsonian agents that cause neuroprotection against haloperidol-induced oxidative stress in mice. Med Chem Res 2009;18:287-308.
3. Azam F. Therapeutic potential of free radical scavengers in neurological disorders. In: Kozyrev D, Slutsky V, editors. Handbook of Free radicals: Formation, Types and Effects. New York: Nova Publishers; 2010. p. 57- 97.
4. Azam F, Alkskas IA, Ahmed MA. Synthesis of some urea and thiourea derivatives of 3-phenyl/ethyl-2-thioxo-2,3-dihydrothiazolo [4,5-*d*]pyrimidine and their antagonistic effects on haloperidol-induced catalepsy and oxidative stress in mice. Eur J Med Chem 2009;44:3889-97.
5. Azam F, Barodia SK, Anwer T, Alam MM. Neuroprotective effect of naphtha[1,2-*d*]thiazol-2-amine in an animal model of Parkinson's disease. J Enzyme Inhib Med Chem 2009;24:808-17.
6. Azam F, Ibn-Rajab IA, Alruiad AA. Adenosine A_{2A} receptor antagonists as novel anti-Parkinsonian agents: A review of structure-activity relationships. Pharmazie 2009;64:771-95.
7. Azam F, El-Gnidi BA, Alkskas IA, Ahmed MA. Design, synthesis and anti-Parkinsonian evaluation of 3-alkyl/aryl-8-(furan-2-yl)thiazolo[5,4-*e*] [1,2,4]triazolo[1,5-*c*]pyrimidine-2(3*H*)-thiones against neuroleptic-induced catalepsy and oxidative stress in mice. J Enzyme Inhib Med Chem 2010;25:818-26.
8. Obeso JA, Olanow CW, Nutt JG. Levodopa motor complications in Parkinson's disease. Trends Neurosci 2000;23 Suppl 10:S2-7.
9. Singer TP. Perspectives in MAO: Past, present, and future. A review. J Neural Transm 1987;23:1-23.
10. Di Monte DA, De Lanney LE, Irwin I, Royland JE, Chan P, Jakowec MW, *et al*. Monoamine oxidase-dependent metabolism of dopamine in the striatum and substantia nigra of L-DOPA-treated monkeys. Brain Res 1996;738:53-9.
11. Finberg JP, Wang J, Bankiewicz K, Harvey-White J, Kopin IJ, Goldstein DS. Increased striatal dopamine production from L-DOPA following selective inhibition of monoamine oxidase B by R(+)-N-propargyl-1-aminoindan (rasagiline) in the monkey. J Neural Transm 1998;52:279-85.
12. Youdim MB, Bakhle Y. Monoamine oxidase: Isoforms and inhibitors in Parkinson's disease and depressive illness. Br J Pharmacol 2006;147 Suppl 1:S287-96.
13. Schwarzschild MA, Agnati L, Fuxe K, Chen JF, Morelli M. Targeting adenosine A_{2A} receptors in Parkinson's disease. Trends Neurosci 2006;29:647-54.
14. Bibbiani F, Oh JD, Petzer JP, Castagnoli N Jr, Chen JF, Schwarzschild MA, *et al*. A_{2A} antagonist prevents dopamine agonist-induced motor complications in animal models of Parkinson's disease. Exp Neurol 2003;184:285-94.
15. Petzer JP, Castagnoli N, Schwarzschild MA, Chen J, Schyf CJ. Dual target–directed drugs that block monoamine oxidase B and adenosine A_{2A} receptors for Parkinson's disease. Neurotherapeutics 2009;6:141-51.
16. Sun H, Scott DO. Structure-based drug metabolism predictions for drug design. Chem Biol Drug Des 2010;75:3-17.
17. Azam F, Prasad MV, Thangavel N, Ali HI. Molecular docking studies of 1-(substituted phenyl)-3-(naphtha[1,2-d]thiazol-2-yl) urea/thiourea derivatives with human adenosine A2A receptor. Bioinformation 2011;6:330-4.
18. Muller CE, Geis U, Hipp J, Schobert U, Frobenius W, Pawlowski M, *et al*. Synthesis and structure-activity relationship of 3,7-dimethyl-1-propargylxanthine derivatives, A_{2A}-selective adenosine receptor antagonists. J Med Chem 1997;40:4396-405.
19. Petzer JP, Steyn S, Castagnoli KP, Chen JF, Schwarzschild MA, Schyf CJ, *et al*. Inhibition of monoamine oxidase B by selective adenosine A_{2A} receptor antagonists. Bioorg Med Chem 2003;11:1299-310.

20. Jacobson KA, Gallo-Rodriguez C, Melman N, Fischer B, Maillard M, Van Bergen A, *et al*. Structure-activity relationships of 8-styrylxanthines as A2-selective adenosine receptor antagonists. J Med Chem 1993;36:1333-42.
21. Shimada J, Koike N, Nonaka H, Shiozaki S, Yanagawa K, Kanda T, *et al*. Adenosine A_{2A} antagonists with potent anti-cataleptic activity. Bioorg Med Chem Lett 1997;7:2349-52.
22. Suzuki F, Shimada J, Koike N, Nakamura J, Shioazaki S, Ichikawa S, *et al*. Therapeutic agent for Parkinson's disease. United States Patent PN/5484920, 1996.
23. Pretorius J, Malan SF, Castagnoli N Jr, Bergh JJ, Petzer JP. Dual inhibition of monoamine oxidase B and antagonism of the adenosine A_{2A} receptor by (*E*,*E*)-8-(4-phenylbutadien-1-yl)caffeine analogues. Bioorg Med Chem 2008;16:8676-84.
24. Cheng YC, Prusoff WH. Relationship between the inhibition constant (K_i) and the concentration of inhibitor which causes 50 per cent inhibition (I_{50}) of an enzymatic reaction. Biochem Pharmacol 1973;22:3099-108.
25. Binda C, Wang J, Pisani L, Caccia C, Carotti A, Salvati P, *et al*. Structure of human monoamine oxidase B, a drug target for the treatment of neurological disorders. J Med Chem 2007;50:5848-52.
26. Jaakola VP, Griffith MT, Hanson MA Cherezov V, Chien YE, Lane JR, *et al*. The 2.6 angstrom crystal structure of a human A_{2A} adenosine receptor bound to an antagonist. Science 2008;322:1211-7.
27. Stewart JJ. Stewart Computational Chemistry, Version 9.03CS. MOPAC 2009. Available from: http://OpenMOPAC.net.
28. Morris GM, Goodsell DS, Halliday RS, Huey R, Hart WE, Belew RK, *et al*. Automated docking using a Lamarckian genetic algorithm and an empirical binding free energy function. J Comput Chem 1998;19:1639-62.
29. Zhao Y, Abraham MH, Lee J, Hersey A, Luscombe NC, Beck G, *et al*. Rate-limited steps of human oral absorption and QSAR studies. Pharm Res 2002;19:1446-57.
30. Ertl P, Rohde B, Selzer P. Fast calculation of molecular polar surface area as a sum of fragment-based contributions and its application to the prediction of drug transport properties. J Med Chem 2000;43:3714-7.
31. Lipinski CA, Lombardo L, Dominy BW, Feeney PJ. Experimental and computational approaches to estimate solubility and permeability in drug discovery and development settings. Adv Drug Deliv Rev 2001;46:3-26.
32. Molinspiration Cheminformatics, Bratislava, Slovak Republic. Available from: http://www.molinspiration.com/services/properties.html. [Last Accessed on 2010 Apr 22].
33. Wang R, Lu Y, Wang S. Comparative evaluation of 11 scoring functions for molecular docking. J Med Chem 2003;46:2287-303.
34. Sawynok J, Liu XJ. Adenosine in the spinal cord and periphery: Release and regulation of pain. Prog Neurobiol 2003;69:313-40.
35. Yuzlenko O, Kiec-Kononowicz K. Molecular modeling of A_1 and A_{2A} adenosine receptors: Comparison of rhodopsin- and β_2-adrenergic-based homology models through the docking studies. J Comput Chem 2008;30:14- 32.
36. Shi Y, Liu X, Gebremedhin D, Falck JR, Harder DR, Koehler RC. Interaction of mechanisms involving epoxyeicosatrienoic acids, adenosine receptors, and metabotropic glutamate receptors in neurovascular coupling in rat whisker barrel cortex. J Cereb Blood Flow Metab 2008;28:111-25.
37. Kim J, Wess J, Van-Rhee AM, Schoneberg T, Jacobson KA. Site-directed mutagenesis identifies residues involved in ligand recognition in the human A2a adenosine receptor. J Biol Chem 1995;270:13987-97.
38. Moro S, Deflorian F, Spalluto G, Pastorin G, Cacciari B, Kim SK, *et al*. Demystifying the three dimensional structure of G protein-coupled receptors (GPCRs) with the aid of molecular modeling. Chem Commun 2003;24:2949-56.
39. Hanson MA, Cherezov V, Griffith MT, Roth CB, Jaakola VP, Chien EY, *et al*. A specific cholesterol binding site is established by the 2.8 Å structure of the human beta2-adrenergic receptor. Structure 2008;16:897- 905.
40. De Colibus L, Li M, Binda C, Lustig A, Edmondson DE, Mattevi A. Three-dimensional structure of human monoamine oxidase A (MAO A): Relation to the structures of rat MAO A and human MAO B. Proc Natl Acad Sci U S A 2005;102:12684-9.
41. Binda C, Li M, Hubalek F, Restelli N, Edmondson DE, Mattevi A. Insights into the mode of inhibition of human mitochondrial monoamine oxidase B from high-resolution crystal structures. Proc Natl Acad Sci U S A 2003;100:9750-5.
42. Binda C, Mattevi A, Edmondson DE. Functional role of the "aromatic cage" in human monoamine oxidase B: Structures and catalytic properties of Tyr435 mutant proteins. J Biol Chem 2002;45:4775-84.
43. Binda C, Newton-Vinson P, Hubalek F, Edmondson DE, Mattevi A. Structure of human monoamine oxidase B, a drug target for the treatment of neurological disorders. Nat Struct Biol 2002;9:22-6.
44. Veber DF, Johnson SR, Cheng HY, Smith BR, Ward KW, Kopple KD. Molecular properties that influence the oral bioavailability of drug candidates. J Med Chem 2002;45:2615-23.

How to cite this article: Azam F, Madi AM, Ali HI. Molecular docking and prediction of pharmacokinetic properties of dual mechanism drugs that block MAO-B and adenosine A_{2A} receptors for the treatment of Parkinson's disease. J Young Pharmacists 2012;4:184-92.

Source of Support: Nil, **Conflict of Interest:** None declared.